

## Effect of Temperature and Microstructure on the Corrosion Behaviour of a Low Carbon Dual Phase Steel

S.C. Ikpeseni<sup>1,2</sup> and E.S. Ameh<sup>2,3</sup>

<sup>1</sup>Department of Mechanical Engineering, Delta State University, P.M.B. 1, Abraka, Oleh Campus, Delta. State, Nigeria.

<sup>2</sup>Department of Mechanical Engineering, University of Benin, Benin City, Edo State, Nigeria.

<sup>3</sup>Mechanical Integrity Department, Chevron Nigeria Limited.

**Abstract:** This work assesses the impact of intercritical annealing temperature and microstructure on the corrosion performance of duplex microstructure steel developed from 0.23%C steel in 0.1M HCl solution. After normalizing, the duplex microstructure was developed through intercritical annealing heat treatment at 730°C, 750°C, 770°C and 790°C respectively for 30minutes and quenched in water. Samples for microscopic examination and corrosion rate measurements were prepared. Optical microscope was used to examine the microstructures. The point count method using stereology was used to evaluate the martensite volume fraction in the developed duplex structure. Weight loss method was used to determine the corrosion rate of the samples in 0.1M HCl. Results obtained showed that the microstructure of the normalized sample was characterized by the presence of alternate layers of pearlite and ferrite, while that of the intercritical annealed samples revealed the presence of dispersed martensite in a ferrite matrix. It was equally observed that the relative amount of martensite in the developed duplex structure increased with increase in annealing temperature. Corrosion rate of the developed dual phase steels was slightly higher than that of the dual phase steel, whereas the corrosion rate of the dual phase steels increased as a function of martensite volume fraction.

**Keywords:** intercritical annealing; temperature; dual phase steel; microstructure; corrosion rate

### I. Introduction

Steel has remained the most widely used and versatile engineering material. As a result it has attracted the attention of many researchers [1 – 11]. Even now more efforts are still geared towards improving the properties of this famous material called “steel”. The energy crisis of mid 1970s coerced the automotive industry to shift attention to lightweight materials in order conserve or optimize fuel consumption. However lofty this idea may be, reliability and integrity of the vehicles as well as the safety of users and environment cannot be compromised. These culminated to the development of a new class of steel known as “Advance High Strength Steels (AHSS)”. This class of steel is further sub divided into dual phase (DP) steel, plastically induced transformation (TRIP) steel, complex phase (CP) steel, ultra high strength steels (UHSS) etc. Among all, dual phase steel is the most popular and thus has attracted the attention of researchers more than any other group. It has wide range of application in the automotive industry and other areas as depicted in Table 1. Good compromise between strength and ductility, as well as improved impact and fatigue properties has made DP steel a popular candidate material for the manufacture of automotive components.

**Table 1:** Range of automotive components build from DP steels (from different Manufacturers) [12]

Producer	Component
General Motors	Wheel discs and rims, bumper reinforcements, face bars, jack posts, water pump pulleys, Steering coupling reinforcements
Hoesch-Estel	Wheel discs
Inland Steel	Plate brake backing (grinding), Panel for doors, deck (boot) lids, centre pillars, windshield frames, wheel houses
Jones and Laughlin	Bumper face bars, bumper reinforcements, rear suspension, wheels, alternator fan blades, steering column reinforcements
Kawasaki	Stylised wheel discs, door and hood panels and fenders
Nippon Steel	Bumper stay/facing door impact bars, frame sections
NKK	Outer and inner panels, door, beam and bumper reinforcements
Sumitomo Metal Industries Ltd	Outer body panels
ToksidAccial	Stylised wheel discs
US Steel	Parts in cars, trucks, buses, farm equipment, industrial handling units, heavy construction units

Examples of applications of DP steel in sectors different from automotive are:

- Precision tubes
- Train seats
- Liquid Petroleum Gas (LPG) cylinders
- Pipes for conveying crude and petroleum products
- Yellow goods (quarrying equipment, earth moving equipment, fork lift trucks and construction materials)

Most of the DP steels produced are from high strength low alloy (HSLA) steels or medium carbon steels. Furthermore, majority of the researches so far conducted on DP steels are on relationships between processing parameters and mechanical properties, with only a few on their corrosion Behaviour [9,10,14,15]. Hence, the trust of this present work is to develop duplex microstructure from plain low carbon steel and assess the effect of the developed duplex structure and intercritical annealing temperature on its corrosion performance.

## II. Materials And Method

The chemical composition of the low carbon steel used as base material is presented in table 2. It was determined using spark spectrometer metal analyzer. Three sparks at different positions were made and the average taken.

**Table 2:** Chemical Composition of the Investigated Steel

Element	C	Si	Mn	S	P	Cr	Ni	Cu	B	Ti	Fe
Weight (%)	0.23	0.20	0.73	0.03	0.03	0.12	0.10	0.27	0.001	0.001	Balance

### 2.1 Design and Development of the Dual Phase

The base material was first normalized at 850°C for 1hr. After which, the normalized material (samples) was grouped into five, four of the groups were subjected to intercritical annealing heat treatment at 730°C, 750°C, 770°C and 790°C ( $\alpha + \gamma$  region) respectively to develop the duplex microstructure, while the other group was left as normalized.

The intercritical annealing process involved heating to  $\alpha + \gamma$  region, soaking for 30 minutes and quenching in water as schematically represented in Fig. 1. The upper and lower critical transformation temperatures were determined using the Andrews formula [1].

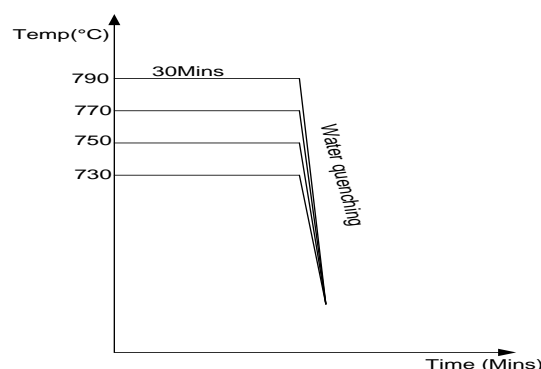


**Fig. 1:** Schematic Illustration of Heat Treatment Schedule for DQ Samples

The samples were given identification codes as shown in Table 3 for easy recognition and in order to avoid mix-ups.

**Table 3:** Sample Identification Codes

Temperature	Normalize	730	750	770	790
Sample Code	A	IAT730	IAT750	IAT770	IAT790

### 2.2 Microstructure Characterization

Samples of both normalized and intercritical annealed steels were prepared for microstructure examination following standard procedures such as sectioning, grinding, polishing and etching [1, 13]. Grinding was carried out with various grits of emery paper, while polishing was done on a rotating wheel covered with sylvect cloth impregnated with 0.2 $\mu$  diamond paste.

Nickon eclipse optical microscope fitted with digital photographic device and computer interface was used to examine the microstructures. After etching with 2% NITAL, ferrite appear light while martensite gray or dark. Thereafter grids were laid on the microstructure photographs and the point count method was used to evaluate

the volume fraction of the phases present [16]. Three specimens were prepared from each sample and five points were examined for each of the specimens and then average taken. The amount of other phases present such as retained austenite or carbide was ignored because its small and negligible.

### 2.3 Corrosion Rate Measurement

Small size coupons were prepared from both normalized and intercritical annealed steel samples for corrosion analysis. The coupons were cut to size, ground and polished using different grits of emery paper, washed in water and rinsed in alcohol and stored under desiccator. Thereafter they were immersed completely in 0.1M HCl solution. The exposure period was 80days while measurements were taken periodically at 8days interval. The weight loss method was adopted; as such the weight of samples before and after exposure to the corrosion environment was measured. Equation (1) [17 – 19] was used to evaluate the corrosion rate.

$$CR = \frac{W}{At}$$

(1)

Where CR = corrosion rate, W = weight loss, A = Total surface area of sample and t = Exposure time. Specific mass loss ( $\text{mg}/\text{cm}^2$ ) was equally evaluated on each monitoring session using equation (2).

$$\text{Specific mass loss} = \frac{W}{A} \quad (2)$$

The above corrosion rate evaluation procedures were in compliance with ASTM G31 standard recommendation practice.

Potential between the sample and the environment was measured on each monitoring day with the aid of DT-830D digital multimeter with zinc electrode as the reference electrode. The measured value was converted to saturated calomel electrode (SCE) using equation (3)[20, 21].

$$SCE(mV) = E(mV) - 1030 \quad (3)$$

Where E = measured potential.

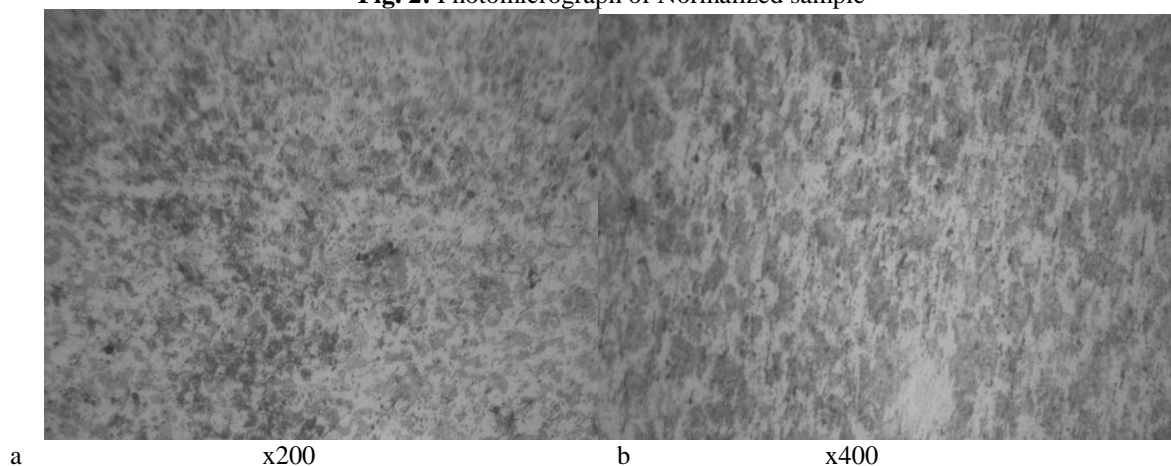
## III. Results And Discussions

### 3.1 Microstructure Characterization Results



X200

Fig. 2: Photomicrograph of Normalized sample



a

x200

b

x400

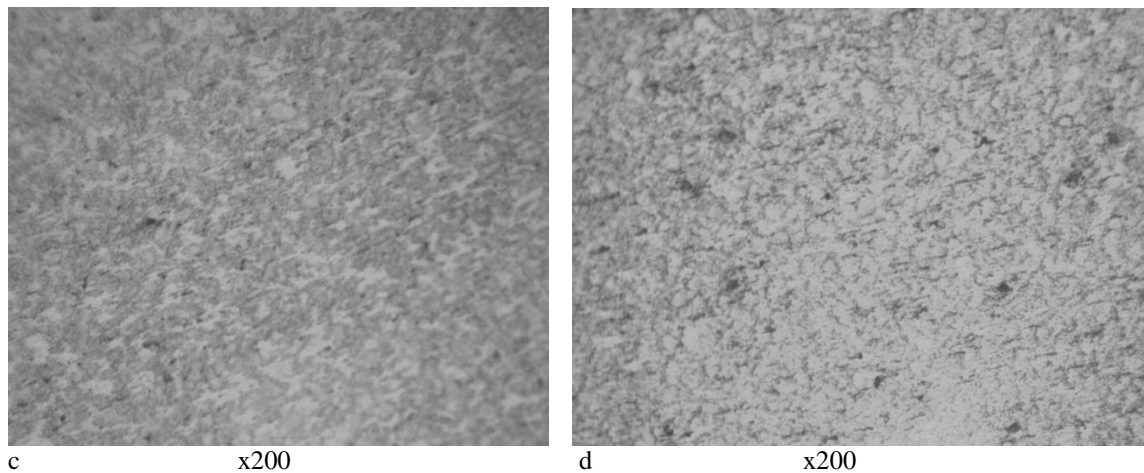


Fig. 3: Photomicrograph of intercritical annealed samples at: (a) 730°C (b) 750°C (c) 770°C (d) 790°C

Figures 2 – 3 are the microphotographs of the structures developed after normalizing and intercritical annealing heat treatments. Figure 2 is the photomicrograph of the normalized sample. It portrays the structure of pearlite (i.e. alternate layers of ferrite [light] and cementite [dark]) and ferrite [light]. Figures 3a – d display the developed dual phase microstructures after intercritical annealing at 730°C, 750°C, 770°C and 790°C accordingly for 30 minutes. The regions shown light is the ferrite while the gray regions represent martensite and some little dark spots retained austenite. The duplex microstructures of the intercritical annealed samples are composed of mainly lath martensite (gray) in an irregularly shaped ferrite (light) matrix. The martensite is found to lie preferably along previous austenite grain boundaries.

Table 4 shows the analysis of the volume fraction of martensite present in the developed duplex microstructure at the corresponding temperatures. It shows that martensite volume fraction increased as a function of temperature. This observation is in agreement with those of Alaneme and Momoh [22]; Bag et al [4] and Dzupon et al [23]. A maximum total standard deviation of ±5 was observed which indicates high reliability of result obtained. At higher temperatures the relative amount of austenite increases which upon quenching transforms to martensite. This accounts for the increase in the volume fraction of martensite as temperature increases.

Table 4: Analysis of Volume Fraction Measurement

Sample	Intercritical Annealing Temperature (°C)	Sample Number	Martensite Volume Fraction [MVF] (%)				Total Average	Total Standard Deviation
			MVF per Sample	Average	Standard Deviation			
IAT730	730	1	16.7,16.7,20.8,12.5,16.7	16.7	±2.6	17	±3	
		2	20.8,25,16.7,20.8,20.8	20.8	±2.6			
		3	16.7,8.3,16.7,8.3,12.5	12.5	±3.3			
IAT750	750	1	16.7,33.3,25,29.2,20.8	25	±5.9	25	±3.7	
		2	20.8,16.7,16.7,20.8,16.7	18.3	±2.0			
		3	25,33.3,29.2,33.3,33.3	30.8	±3.0			
IAT770	770	1	41.7,25,33.3,37.5,29.2	33.3	±5.9	33	±5	
		2	29.2,41.7,29.2,37.5,37.5	35	±5.0			
		3	25,37.5,29.2,33.3,33.3	31.7	±4.2			
IAT790	790	1	41.7,37.5,45.8,37.5,45.8	41.7	±3.7	38	±3.7	
		2	41.7,33.3,37.5,37.5,45.8	39.2	±4.4			
		3	33.3,37.5,29.2,29.2,33.3	32.5	±4.2			

3.2 Corrosion Rate Results

Figs.4 and 5 show the plots of specific mass loss and corrosion rate against exposure time respectively. Figs.6 and 7 show the graphs of specific mass loss and corrosion rate against intercritical annealing temperature respectively; while the plots of specific mass loss and corrosion rate versus martensite volume fraction are presented in Figs. 8 and 9 respectively. Fig. 10 shows the graph of electrode potential (SCE) against exposure time.

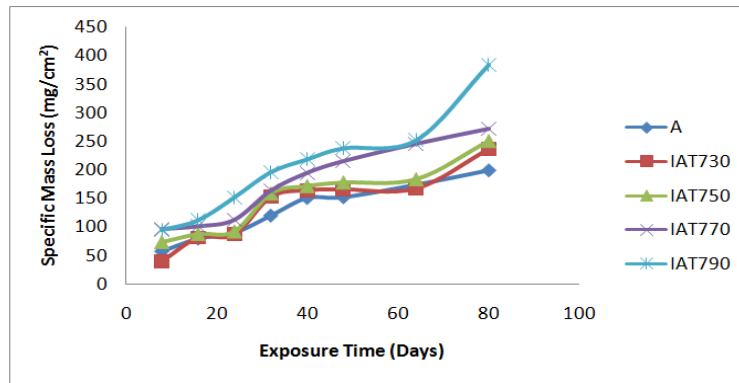


Fig. 4: Specific Mass Loss versus Exposure Time

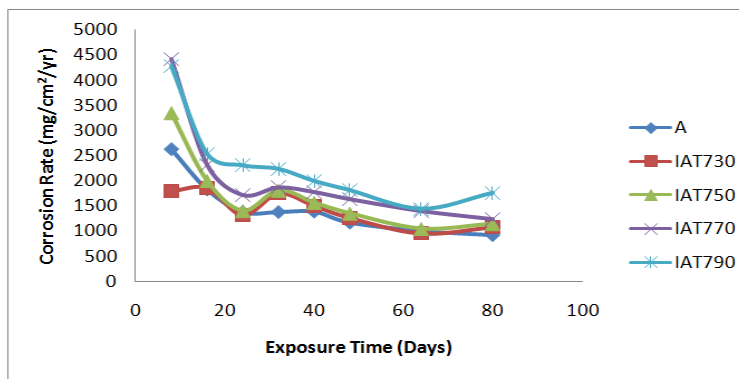


Fig. 5: Corrosion Rate versus Exposure Time

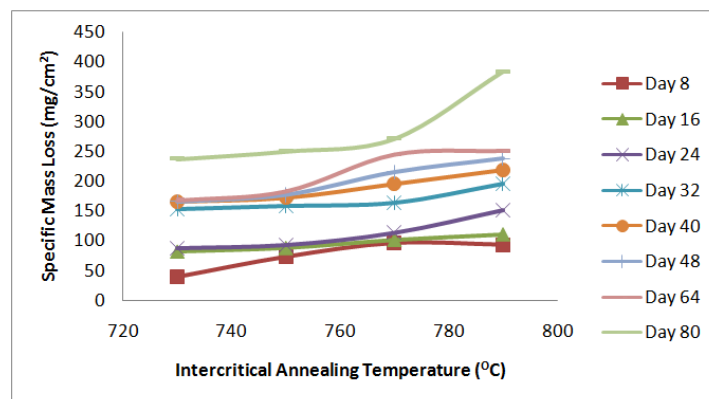


Fig. 6: Specific Mass Loss versus Intercritical Annealing Temperature

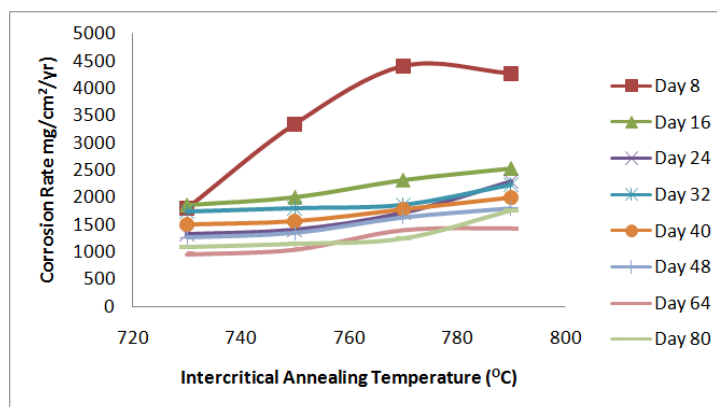


Fig. 7: Corrosion Rate versus Intercritical Annealing Temperature

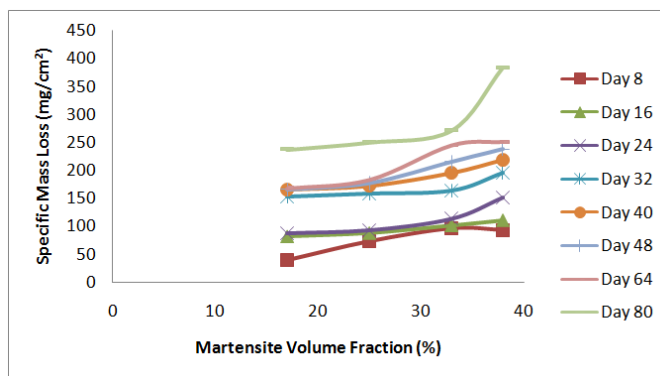


Fig. 8: Specific Mass Loss versus Martensite Volume Fraction

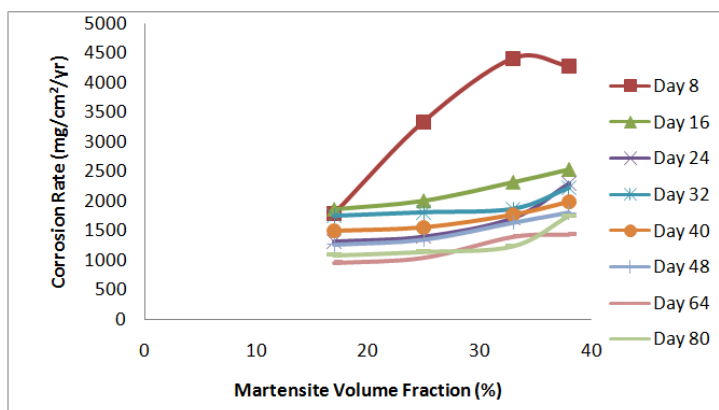


Fig. 9: Corrosion Rate versus Martensite Volume Fraction

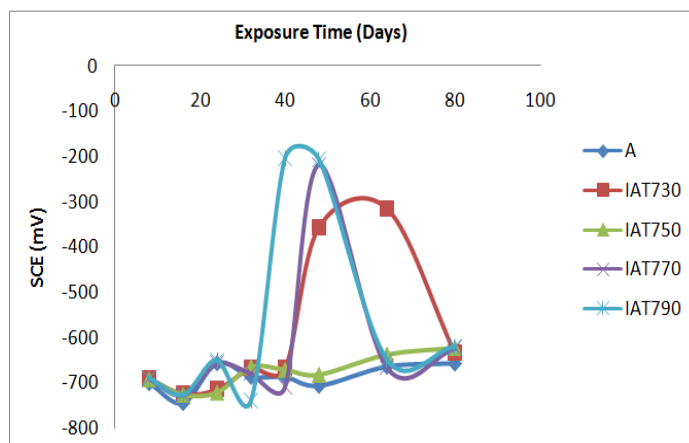


Fig. 10: SCE versus Exposure Time

It is clearly demonstrated that specific mass loss (i.e. mass loss per unit area) increased with increase in exposure time, while corrosion rate decreased rapidly at the initial time and thereafter rate of decrease in corrosion rate reduced. Both mass loss and corrosion rate were higher for the dual phase steels than the normalized steel. The reduction in the rate of corrosion could be attributed to partial protection offered by corrosion products. This can be corroborated with Fig. 10 as the electrode potential shifts towards the passive region with increased exposure time. This passive tendency is due to the partial passivation from corrosion products (oxide films) formed on the surface of the metal (samples).

Both specific mass loss and corrosion rate increased as intercritical annealing temperature increases – Figs. 6 and 7. Similarly, specific mass loss and corrosion rate increased as a function of martensite volume fraction – Figs. 8 and 9. As earlier stated, at higher intercritical annealing temperatures, the relative amount of austenite increases which upon quenching transforms to martensite, hence, the relative amount of martensite in the duplex microstructure increases with increased intercritical annealing temperature. Upon exposure to the corrosive environment (i.e. 0.1M HCl), martensite becomes cathodic while ferrite becomes anodic to the

microgalvanic corrosion cells that are set up. As the martensite volume fraction increases an unfavorable (increased) cathode to anode area ratio is set up which leads to rapid dissolution of the ferrite phase and thus increased corrosion rate with increased amount of martensite.

Generally, the corrosion rate of the dual phase steels was slightly higher than that of normalized steel.

#### IV. Conclusion

In this research it has been established that the corrosion rate of dual phase steel developed from 0.23%C steel via intercritical annealing heat treatment increases with increase in intercritical annealing temperature and martensite volume fraction in 0.1M HCl solution. It was also revealed that martensite volume fraction increases as a function of temperature. Again, the corrosion rate of the duplex microstructure steels was found to be slightly higher than that of normalized steel.

#### References

- [1]. Ikpeseni S.C., Onyekpe B.O. and Momoh I.M., Effect of tempering on the microstructure and mechanical properties of austenitic dual phase steel, *International Journal of Physical Sciences*, 10(16), 2015, 490 – 497.
- [2]. Ikpeseni S.C., Onyekpe B.O. and Ovri H., Influence of intercritical annealing temperature on mechanical properties and microstructure of 0.23% C low alloy steel, *Nigerian Journal of Technology (NIJOTECH)*, 349(3), 2015, 499 – 505.
- [3]. Ovri H. and Kamma C.M., Evaluation of the transformation mechanisms and mechanical properties of ferrite-martensite microalloyed steels, *Materials Research*, 11(1), (2008), 97 – 101.
- [4]. Bag, A.; Ray, K.K. and Dwarakadasa, E.S., Influence of martensite content and morphology on tensile and impact properties of high-martensite dual-phase steels, *Metallurgical and Materials Transactions A*, 30 (5): 1193-1202.
- [5]. Offor P.O., Ezekoye V.A. and Ezekoye B.A. (2010): Influence of heat treatment on the mechanical properties of 0.13wt% structural steel, *The Pacific Journal of Science and Technology*, 11 (2), 1999, 16 – 21.
- [6]. Panda, S.K.; Hernandez, V.H.B.; Kuntz, M.L. and Zhou, Y., Formability analysis of diode-laser-welded tailored blanks of advanced high-strength steel sheets, *Metallurgical and Materials Transactions A*, 40A (8), 2009, 1955-1967.
- [7]. Hilditch, T.; Timokhina, I.; Robertson, L.; Pereloma, E. and Hodgson, P., Cyclic Deformation of advanced high-strength steels: mechanical behavior and microstructural analysis, *Metallurgical and Materials Transactions A*, 40A (2), 2009, 342-353.
- [8]. Wu, D.; Li, Z. and Lue, H.S., Effect of controlled cooling after hot rolling on mechanical properties of hot rolled trip steel, *Steel Research International*, 15 (2), 2008, 65-70.
- [9]. Hadzipasic A.B., Hadzipasic H. and Vrbnjac S., The influence of medium and microstructure on corrosion rate of dual phase high-strength structural steels, *The Holistic Approach to Environment*, 2(2), 2012, 73 -74.
- [10]. Sarkar, P.P., Kumar P. and Chakraborti P.C., Microstructural influence on the electrochemical corrosion behaviour of dual-phase steels in 3.5% NaCl solution, *Materials Letters*, 59(19-20), 2005, 2488-2491.
- [11]. Korzekwa, D.A.; Lawson, R.D.; Matlock, D.K. and Krauss, G., A consideration of models describing the strength and ductility of dual-phase steels, *Scripta Metallurgica*, 14 (9), 1980, 1023-1028.
- [12]. Llewellyn, D.T. and D.J. Hillis, Dual phase steels, *Ironmaking and Steelmaking*, 23(6), 1996, 471-478.
- [13]. Davies, R.G., Influence of martensite composition and content on properties of dual phase steels, *Metallurgical Transactions A*, 9 (5), 1978, 671-679.
- [14]. Chen, Y.Y., Tzeng H.J., Wei L.I., and Shili H.C., Corrosion resistance and mechanical properties of low-alloy steels under atmospheric conditions, *Corrosion Science*, 47(4), 2005, 1001-1021.
- [15]. Trejo, D., et al., Mechanical-properties and corrosion susceptibility of dual-phase steel in concrete, *Cement and Concrete Research*, 24(7), 1994, 1245-1254.
- [16]. Russ J.C. and Dehoff R.T., *Practical stereology* (New York, Plenum Press, 2<sup>nd</sup> Ed, 1999).
- [17]. Fontana M.G., *Corrosion engineering* (New Delhi, Tata McGraw-Hill, 3<sup>rd</sup> ed., 2007).
- [18]. Ogunleye, I.O.; Adeyemi, G.J.; Onyegoke, A.O.V., Effect of grape fruit juice on the corrosion behaviour of mild steel in acidic medium, *American Journal of Scientific and Industrial Research*, 2 (4), 2011, 611 – 615.
- [19]. Olorunfoba D.T., Ogunniyi I.O. and Fabuyide A.A., Nickel plating and cathodic protection for low carbon steel in chloride environment, *NSE Technical Transactions*, 47 (2), 2013, 29 - 38.
- [20]. Afolabi A.S. and Fasuba O.A., Corrosion of steel reinforcement in concrete immersed in different environments, *NSE Technical Transactions*, 41 (4) 2006, 51 – 60.
- [21]. Hilbert O.B. and James A.M., *Dictionary of electro-chemistry* (London, Macmillan press, 1984).
- [22]. Alaneme K.K. and Momoh I.M., Mechanical properties and corrosion behaviour of micro-duplex medium carbon low alloy steel, *International Journal of Engineering*, 12, 2014, 386 – 392.
- [23]. Dzupon M., Parilak L. Kollarova M. and Sinaiova I., Dual phase ferrite – martensitic steel micro-alloyed with V- Nb, *Metabk*, 46(1), 2007, 15-20.